Research Square

Preprints are preliminary reports that have not undergone peer review.
They should not be considered conclusive, used to inform clinical practice,
or referenced by the media as validated information.

Unravelling key drivers of Ostreid herpesvirus type 1 (OsHV- 1) transmission dynamics in Pacific oysters through a data-driven epidemiological modeling approach

Jules Trillaud
Ifremer
Coralie Lupo
Ministry of Agriculture
Benjamin Morga
Ifremer
Nicole Faury
Ifremer
Bruno Petton
Ifremer, UBO, CNRS, IRD
Tristan Renault
Ifremer
Isabelle Arzul
Ifremer
Maude Jacquot
maude.jacquot@ifremer.fr

Ifremer

Research Article

Keywords: OsHV-1, Herpesvirus, Magallana gigas, Epidemiological modelling, Aquaculture, Mollusk diseases, Oyster mortality, Approximate Bayesian Computation, Sensitivity analysis

Posted Date: April 7th, 2026

DOI: https://doi.org/10.21203/rs.3.rs-9246047/v1

License: This work is licensed under a Creative Commons Attribution 4.0 International License.
Read Full License

Additional Declarations: No competing interests reported.

Abstract

Over the past few years, methodological advances have driven major progress in epidemiological modelling tools, improving our ability to understand pathogen dynamics and inform management strategies. However, these powerful approaches remain underused in marine mollusc health, despite their well-recognized potential to assess the impact of pathogens that threaten the long-term viability of the industry. This is notably the case for Ostreid herpesvirus type 1 (OsHV-1), a virus associated with recurrent mass mortalities of Pacific oyster spat worldwide. These recurring outbreaks underscore important gaps in our understanding of its transmission dynamics and the strategies required to mitigate epizootic events. To bridge this gap, we developed a stochastic compartmental epidemiological model that extends the classical SEIR framework by incorporating an environmental viral compartment and distinguishing between oysters that survive infection and those that succumb to it. Model parameters were estimated using targeted experimental data and integrated into stochastic simulations, enabling the model to reproduce the overall dynamics of the observed mortality kinetics and thereby supporting its validity. Remaining discrepancies were then addressed using an Approximate Bayesian Computation approach to refine parameter estimates and improve model accuracy. Additionally, sensitivity analysis identified viral shedding rates as the main drivers of epidemic dynamics. Through this integrative framework, we provide new insights into OsHV-1 transmission patterns and establish a foundation for future spatial modelling aimed at supporting disease management in oyster farming.

INTRODUCTION

In 2022, the global production of farmed aquatic animals reached 94 million tonnes (FAO, 2024). Mollusk accounted for 20% of this production, led by the Pacific oyster, *Magallana gigas* (formerly *Crassostrea gigas*), generating revenues exceeding 1.5 billion US dollars in the same year (FAO, 2024). However, despite overall growth, this production has decreased in certain countries. In France, for example, it has steadily declined at an average rate of 0.05% per year since 1950 (Botta et al., 2020). Although influenced by multiple factors, this decline mainly reflects historical and ongoing health challenges faced by the oyster industry, inducing substantial economic losses and concerns for producers and coastal activities (Girard & Pérez Agúndez, 2014). Among these, the Ostreid HerpesVirus type 1 (OsHV-1) (Davison et al., 2005; Renault, 2024) stands out as a central issue, causing reccurrent annual mortality in Pacific oyster spat, leading to losses ranging from 40% to 100% in affected regions (Garcia et al., 2011; Renault, Cochennec, et al., 1994; Renault, Le Deuff, et al., 1994; Segarra, 2014).

OsHV-1 was first identified in France in the early 1990s following unexpected mortality events among Pacific oyster spat (Renault et al., 1995; Renault, Le Deuff, et al., 1994). These outbreaks rapidly extended beyond France, and the virus, along with several of its variants, was subsequently detected in Pacific oyster farming areas worldwide (Hwang et al., 2013; Jenkins et al., 2013; S. E. Keeling et al., 2014; Renault et al., 2012). In 2008, a marked shift in viral infection distribution was observed in France, with nearly all production sites reporting spat mortality rates ranging from 80 to 100% within a few days (EFSA, 2010). This unprecedented increase in mortality was associated with the emergence of an OsHV-

1 variant designated as OsHV-1 µVar (Segarra et al., 2010). Since then, this variant has remained highly virulent, causing recurrent outbreaks when seawater temperatures exceed approximately 16°C (Alfaro et al., 2019; Renault et al., 2014). OsHV-1 is transmitted throught waterborne pathways following the release of viral particles by infectious oysters in seawater (Schikorski, Faury, et al., 2011; Schikorski, Renault, et al., 2011a). The virus primarily affects larvae, spat (< 6 months old), and juvenile oysters (6–12 months old), which experience substantially higher mortality rates than adults (Green et al., 2016; P. M. Hick et al., 2018; Segarra, Baillon, et al., 2014).

Studies investigating interactions between OsHV-1 and its host have highlighted inter-individual variability in resistance to infection, with some oysters able to limit viral replication and survive infection (Dégremont, 2011; Dégremont et al., 2010). Among the factors involved, host genetics has emerged as a major determinant of this resistance (Azéma et al., 2017; Dégremont, Lamy, et al., 2015; Dégremont, Nourry, et al., 2015). However, the high costs associated with research and genetic selection constrain both the large-scale implementation and evaluation of breeding programs (Delomas et al., 2023). In addition, the oyster production cycle, which lasts approximately three years and relies on both wild-caught and hatchery-produced spat, is characterized by a diversity of zootechnical practices and numerous transfers between sites at different growing stages. This structural complexity, together with the range of stakeholders involved, makes the development of effective and sustainable OsHV-1 mitigation strategies particularly challenging. Given these issues, epidemiological modelling stands out as a particularly suitable and adapted approach, enabling a deeper understanding of infection dynamics, evaluating risks, and assessing the effectiveness of potential management strategies to guide decision-making (M. J. Keeling & Rohani, 2008; Pernet et al., 2016; Renault, 2024).

Modeling approaches are widely used to study pathogen dynamics, not only in human health (Marques et al., 2021; Tang et al., 2020), but also in livestock species (Doeschl-Wilson, 2011; Siettos & Russo, 2013). In aquatic production systems, adaptations of the Susceptible, Exposed, Infectious, Recovered (SEIR) framework (Kermack & Mckendrick, 1927) have been applied to both wild fish populations (Giménez-Romero et al., 2021; Murray et al., 2001) and aquacultured fish species (Murray, 2013; Salama & Murray, 2013). In the context of marine mollusk diseases, the availability of epidemiological models remains relatively scarce. Nevertheless, specific models have been developed to examine the dynamics of pathogens such as the parasite *Perkinsus marinus* in *Crassostrea virginica* (Bidegain et al., 2017) and the bacterium *Vibrio aestuarianus* in *M. gigas* (Lupo et al., 2019). Similary, only a few studies have explored modeling approaches for OsHV-1, both within populations of *M. gigas* (Ferreira et al., 2021) and in co-culture systems involving *M. gigas* and *Crassostrea virginica* (Adekunle et al., 2025). These studies provide a basis for exploring the epidemiological dynamics of OsHV-1 by calibrating, respectively, a Susceptible, Exposed, Infectious, Dead (SEID) and a Susceptible, Infectious, Dead (SID) model. However, none of the existing models account for host survival following infection, a key factor influencing OsHV-1 dynamics that exhibits considerable variation across oyster populations (Dégremont et al., 2016). Accounting for this biological trait is essential for realistic epidemiological modeling and supports the inclusion of a R compartment, as in SEIR models, to represent indiviuals surviving infection and their effect on transmission dynamics. Furthermore, parameters estimates used in the existing models

derived from diverse literature sources and therefore may reflect OsHV-1 µVar of different origins, likely corresponding to different microvariants. This is particulary important because such variants have been shown to induce distinct responses within the same oyster population (Agnew-Camiener et al., 2026; Friedman et al., 2020). Consequently, model calibration should be performed specifically for the microvariant under study in order to improve predictive accuracy and capture specific epidemiological patterns of a geographic region.

In this context, we developed a compartmental model to simulate the dynamics of OsHV-1 µVar in *M. gigas* populations and calibrated its parameters using OsHV-1 µVar viruses isolated from the Marennes-Oléron Bay in 2014. Our objectives were to i) adapt the SEIR model structure by introducing two distinct pathways to differentiate between oysters that survive or succumb to infection, ii) estimate model parameter values using dedicated experimental data in combination with Approximate Bayesian Computation (ABC) inference techniques and iii) conduct a sensitivity analysis to identify the parameters that most influence disease dynamics and model outcomes.

MATERIAL AND METHODS

Adaptation of the SEIR compartmental model

We developed a Susceptible, Water, Exposed, Infectious, Recovered and Dead (SWEIRD) model extending the classical SEIR framework, by explicitly incorporating OsHV-1 concentration (*W*) and by distinguishing oysters that survive or succumb to the infection, through separate pathways leading to the Recovered (*R*) or Dead (*D*) compartment, respectively **(**Fig. 1**)**. As virus transmission occurs through direct waterborne exposure, the infection rate of susceptible oysters (*S*) is defined as the infection probability β (1).

$$\beta = \frac{W}{W + K} \quad (1)$$

This probability is modeled with a logistic dose-response function, capturing the non-linear relationship between the viral concentration in seawater (*W*) and the infection probability to better represent transmission dynamics. This function is derived from the well-established Hill equation (Hill et al., 1910) where *K* refers to the 50% infectious concentration, defined as the concentration resulting in a 50% probability of infection. The infected oysters are distributed between the two distinct pathways based on *Φ*, the probability of an oyster to survive the infection. Oysters that will survive progress from the exposed (infected not yet infectious) stage (E_1) to the infectious stage (I_1) before ultimately transitioning to the recovered compartment (*R*). In contrast, oysters that will succumb to infection progress from the exposed compartment (E_2) to the infectious compartment (I_2) and then enter a transient compartment of recently deceased oysters (D_w) that continue to shed viral particles, before reaching the final dead compartment (*D*) which no longer contributes to the evolution of viral concentration in seawater. All inter-compartmental transition rates in the model are governed by parameters estimated from experimental approaches.

Experimental data acquisition for model parameter calibration and validation

Several experimental infection approaches were implemented to estimate the model parameters, either as value distributions or as single-point values (Table 1). Moreover, these parameters were estimated using a viral suspension prepared from dead oysters collected in Marennes-Oléron Bay in 2014, according to a previously published protocol (Schikorski, Renault, et al., 2011a).

Table 1
Estimation and implementation of SWEIRD model parameters

Symbol	Meaning	Estimation approach	Estimation used	Sample size	Stochasticity
Φ	**Probability of an oyster to survive infection**	**Mean survival rate of the validation experimental data**	**Single estimation**	**NA**	**Multinomial draw**
β	Probability of a susceptible oyster to become infected	Logistic dose-response function	Estimation at each step	NA	Binomial draw
K	Concentration of virus that yields a 50% chance of becoming infected	Regression between infection rate and log-transformed injected dose	Single estimation	1	No
ρ_1	Latent period of oysters that survive infection	Time between virus injection and detection in the tank for oyster that survive infection	Density function	11	Density + Binomial draw
ρ_2	Latent period of alive oysters that succumb to infection	Time between virus injection and detection in the tank for oysters that succumb to infection	Density function	39	Density + Binomial draw
γ	Infectious period of oysters that survive infection	Virus detection period for oysters that survive infection	Density function	11	Density + Binomial draw
δ_1	Infectious period of alive oysters that succumb to infection	Virus detection period till death for oysters that succumb to infection	Density function	39	Density + Binomial draw
δ_2	Infectious period of dead oysters	Delay before removing dead oysters in the validation experimental setup	Single estimation	NA	Binomial draw
ω_1	Virus shedding rate of infectious oysters that survive infection	Experimental volume × concentration of virus for infectious oysters that survive infection / time spent in tank	Density function	15	Density + Poisson draw
ω_2	Virus shedding rate of alive oysters that succumb to infection	Experimental volume × concentration of virus for infectious alive oyster that succumb to infection / time spent in tank	Density function	45	Density + Poisson draw

Symbol	Meaning	Estimation approach	Estimation used	Sample size	Stochasticity
Φ	**Probability of an oyster to survive infection**	**Mean survival rate of the validation experimental data**	**Single estimation**	**NA**	**Multinomial draw**
ω_3	Virus shedding rate of infectious dead oysters	Experimental volume × concentration of virus for infectious dead oysters / time spent in tank	Density function	7	Density + Poisson draw
ε	Rate of viral particles inactivation	Proportion of viral particles that become non-infectious within one hour	Single estimation	1	Poisson draw
V	Volume of the simulation environment	Volume of the validation experimental setup	Single estimation	NA	No

The first experimental approach was designed to estimate, latent periods, *i.e.* the time required for infected oysters to become infectious (ρ_1 and ρ_2), infectious periods (γ and δ_1), and viral shedding rates (ω_1 and ω_2) **(Supplementary Fig. 1A)**. To this end, a group of 63 specific pathogen-free Pacific oyster spats produced in Ifremer hatcheries (mean weight of 3.39 g) were injected with 100 µL of a viral suspension, at a concentration of 2.2 x 10^5 copies of DNA per μL^{-1} ($cp.\mu L^{-1}$) in the adductor muscle and placed individually in 1 L tanks containing UV-filtered seawater at 22°C. The water was renewed at an average interval of 24 hours, with a 1.5 mL water sample being collected and undergoing quantitative polymerase chain reaction (qPCR) analysis at each renewal in order to assess viral DNA concentration (see above for more details). Monitoring was conducted for a maximum of 13 days post-injection (dpi), stopping upon the death of the oyster.

A second, similar experimental approach was implemented to obtain data for estimating the shedding rates of dead oysters (ω_3) **(Supplementary Fig. 1B)**. A total of 10 specific pathogen-free Pacific oyster spats produced in Ifremer hatcheries (mean size of 4 cm) were injected with 100 µL of a 2.5 × 10^7 $cp.\mu L^{-1}$ viral suspension in the adductor muscle and subsequently maintained individually in 1 L tanks containing UV-filtered seawater at 22°C. Upon their death, oysters were maintained in the tank, and daily 1 mL water samples were collected for up to 7 dpi. The samples were then analyzed using qPCR to quantify the viral DNA concentration in the tank on each sampling day.

A third experimental approach was implemented to estimate the concentration required to infect 50% of oysters (K) **(Supplementary Fig. 1C)**. In this experiment, 80 specific pathogen-free Pacific oyster spats produced in Ifremer hatcheries (mean size of 4 cm) were injected with 100 µL of a viral suspension at 8 different concentrations, *i.e.* 8 different doses of virus, with 10 oysters per concentration level. These suspensions were obtained through serial dilutions of viral solutions, and the concentrations were quantified using propidium monoazide (PMA) qPCR (see above). Oysters were then injected with

suspensions ranging from 6.14×10^{2} to 1.00×10^{-1} cp.µL⁻¹ and placed in clean tanks containing 0.5 L of UV-treated, filtered seawater maintained at 22°C. Seawater samples of 1 mL were collected daily from each tank for 7 dpi to monitor infection rate using PMA qPCR.

A fourth experimental approach was implemented to estimate the inactivation rate of viral particles in seawater (ε) **(Supplementary Fig. 1D)**. To this end, seawater enriched with viral particles was prepared by injecting Pacific oysters with 100 µL of a 3.23×10^{5} cp.µL⁻¹ viral suspension. After being left to rest for different durations (0, 2, 4, 8, 12, 16, and 20 hours), this contaminated water was then used to expose groups of 10 specific pathogen-free Pacific oyster spats produced in Ifremer hatcheries (mean size of 2.5 cm) at 20°C for 10 days. Mortality was monitored daily for each group and the oyster survival rate at the end was used to provide an estimation of the viral concentration at the begining of the exposure using the Hill equation and the estimated K value. These estimated concentrations were then regressed against resting time using a linear model to determine the slope coefficient, which was subsequently used to estimate the viral particle inactivation rate in seawater under constant and controlled conditions.

Finally, a complementary experimental setup was employed to generate data for model validation. Five 3 L tanks of seawater were prepared, each maintained at 22°C and containing 10 oysters (including one injected with with 100 µL of OsHV-1 suspension) originating from Ifremer hatcheries (mean size of 3 cm). Over a 7-day period, oyster survival was monitored daily, and any dead oysters were removed from the tanks on a daily basis.

DNA extraction, OsHV-1 quantification and data processing

Total DNA was extracted from seawater samples according to a previously described protocol (Pepin et al., 2008) using virus-specific primers pairs targeting a region of the OsHV-1 µVar genome predicted to encode a DNA polymerase catalytic subunit (Webb et al., 2007). Amplification specificity was verified by melting curve analysis, and absolute viral quantification was determined by comparing Ct values with a standard curve generated from an amplicon cloned into the pCR4-TOPO vector for OsHV-1 µVar. Additionally, except for the estimation of K, PMA treatment, which allows the selective quantification of DNA copies associated with intact viral capsids only, was not applied prior to amplification. Consequently, the parameters were estimated from qPCR measurements reflecting viral DNA concentrations rather than concentrations of infectious viral particles (Renault et al., 2024). Despite the biases introduced by these approximations, viral DNA quantification results were considered throughout this study as proxies for the number of infectious particles in order to simplify model formulation and facilitate interpretation. Moreover, to reduce bias associated with qPCR measurement uncertainty, a detection threshold of 4 cp.µL⁻¹ was applied to all water samples, and values below this threshold were set to zero (Pepin et al., 2008). Then, only data from oysters that exhibited detectable viral shedding and subsequently either recovered (remained alive with no further detectable shedding) or died during the experiment were retained for the analysis, allowing individuals to be classified as surviving or succumbing following infection. Finally, for the experimental approach without daily water renewal, viral

shedding rates were estimated from daily variations in viral DNA concentrations. Differences in viral copy numbers between consecutive water samples collected at times t and $t–1$ were calculated, and positive differences were interpreted as net viral release into the water. These values were converted into total viral DNA copies using the experimental volume and subsequently expressed as hourly excretion rates based on the sampling interval.

Accounting for experimental variability into a stochastic framework

Introducing stochasticity into the modeling framework is essential to account for intrinsic random fluctuations and biological variability among individuals. Moreover, this is particularly important in small populations, where individual-level fluctuations do not average out and can substantially affect the overall system dynamics. Because our study focuses on small sample-sizes, stochasticity was incorporated into model transitions to better reflect the inherent variability of the system.

The distributions of the latent periods (ρ_1 and ρ_2), the infectious periods (γ and δ_1) and viral shedding rates (ω_1, ω_2 and ω_3) were compared to normal, log-normal and gamma distributions using the Akaike Information Criterion (Akaike, 1974) to identify the best fitting density function. The resulting probability density functions were then incorporated into the model to randomly assign parameter values at the beginning of each simulation, thus introducing a stochastic component that captures inter-individual variability (Table 1). Moreover, to introduce a second stochastic layer accounting for intra-individual variability, a counterpart of the model's ordinary differential equation system was implemented in discrete-time with a 1-hour time step. The transition rates (r_{ij}) between oyster compartments i and j were converted into transition probabilities (p_{ij}) using the expression $p_{ij} = 1 - exp(- r_{ij})$. The number of individuals transitioning from compartment i to compartment j (N_{ij}) was then drawn from a Binomial distribution: $N_{ij} \sim Binomial\ (C_i, p_{ij})$, where C_i represents the number of individuals in compartment i. For rates associated with virus shedding (rs_i), the number of OsHV-1 particles shed from compartment i at each time step (S_i) was drawn from a Poisson distribution: $S_i \sim Poisson\ (C_i \times rs_i)$, where C_i is still the number of individuals in compartment i. The number of viral particles from oysters of each compartement is then divided by the simulation volume (V) to determine its specific contribution to the overall viral concentration. Moreover, since all compartment contributions are expressed relative to the same volume (V), they can be directly summed to the global viral concentration from the previous time step. The result is then corrected for the proportion of inactivated particles to obtain the updated viral concentration in W.

Parameters not associated with a distribution (Φ, K, δ_2, and ε) were fixed to single values derived from experimental estimation. However, stochasticity was still introduced for the decay rate of viral particles (ε) and the infectious period of dead oysters (δ_2), using a Poisson and a Binomial draw, respectively. Stochasticity was also incorporated into the infection process by applying a Binomial draw using β to determine the number of individuals moving from the susceptible compartment (S) at each time step (Table 1).

Initial settings for model simulation and comparison with validation data

In this study, all simulations were initialized identically to replicate the conditions under which the model validation data were obtained, allowing direct comparison between model outputs and observed oyster mortality kinetics. Each simulation began with nine susceptible oysters and one infected individual. Several key parameters were fixed: the probability of an oyster surviving infection (Φ) was set to 0.375 (reflecting the 37.5% survival rate observed in validation data), the infectious period of dead oysters (δ_2) was set to 24 hours (corresponding to the daily removal of dead individuals in the experimental setup) and the simulation volume (V) was fixed at 3 L to reproduce the conditions of the validation experiment (Table 1).

Using this standardized initialization, we first conducted 1,000 simulations and aggregated the outputs to perform an initial comparison with the validation data. This allowed us to assess the model's ability to reproduce observed patterns before refining parameter estimates through an Approximate Bayesian Computation (ABC) approach. The model was implemented in R (R Core Team, 2023), using the *dplyr* (Wickham et al., 2014) and *tidyr* (Wickham, Vaughan, et al., 2025) packages for data manipulation and *ggplot2* (Wickham, Chang, et al., 2025) and *reshape2* (Wickham, 2025) packages for visualization.

Model validation following ABC parameter adjustment

An ABC framework was then employed to refine model parameter distributions by comparing simulated outputs with observed data (Beaumont et al., 2002; Csilléry et al., 2010). To reduce the computational cost and time typically associated with this type of approach, we adopted the adaptive ABC iterative algorithm (Lenormand et al., 2013), which estimates the posterior distribution of each parameter by progressively sampling from a series of intermediate distributions, thereby refining parameter estimates according to the observed data. At each iteration, parameter sets are sampled from the previous iteration's distributions, and simulation errors are computed by comparing the aggregated mortality kinetics from 10 simulations per parameter set with the observed data. Only sets below a dynamically updated threshold (the 20th percentile of previously accepted errors) are retained. This process continues until 1,000 accepted sets are collected, forming updated parameter distributions progressively focusing on sets producing simulations that better fit the observed data. The algorithm terminates when the proportion of accepted simulations falls below 1%, indicating that further iterations are unlikely to significantly improve the model's accuracy.

For the initialization of this approach, we used densities derived from the experimental data as prior distributions. However, for parameters estimated as point values, we calculated confidence intervals using a bootstrap procedure with 1,000 iterations (Efron & Tibshirani, 1994) for K and using the delta method (Oehlert, 1992) implemented in the *car* package in *R* (Fox et al., 2024) for ε. These confidence intervals ($CI = [CI_1, CI_2]$) were then used to define normal prior distributions for each parameter, setting the mean equal to the point estimate and the standard deviation as $\sigma = (CI_2 - CI_1) / (2 \times 1.96)$. The factor

1.96 corresponds to the 97.5th percentile of the standard normal distribution, ensuring that the resulting normal distribution matches the 95% confidence interval.

The final parameter distributions obtained from the ABC approach were used to perform 1,000 new simulations, which were then aggregated to validate the model and the parameter calibration by comparing the simulated mortality with the observed data. This approach and the resulting final model was also implemented in R (R Core Team, 2023), using the same packages for data manipulation and visualization as previously presented.

Exploring parameter influence through sensitivity analysis

A sensitivity analysis using the Morris method (Morris, 1991) and the *sensitivity* package (Iooss et al., 2025) was performed to assess the effect of individual parameter variations on model dynamics while keeping the computational cost low (Wu et al., 2013). The method was applied generating 100 random trajectories across the parameter space (10 discrete levels, grid jump = 2), varying one parameter at a time, and performing 100 simulations per parameter set to estimate the effect of individual parameter variations on model outputs. We used the 95% confidence intervals of the posterior distributions obtained from the ABC approach to define the lower and upper bounds for each parameter and parameters not experimentally estimated (δ_2 and Φ), were included using bounds relative to values derived from validation data **(**Table 2**).**

Table 2
SWEIRD model calibrated parameters and their sampling ranges for sensitivity analysis

Symbol	Unit	Mean	Lower bounds	Upper bounds
Φ	**NA**	**NA**	**0.1**	**0.9**
K	$cp \cdot \mu L^{-1}$	67.0	3.7×10^{-1}	2.4×10^{2}
ρ_1	h	38 .3	9.1	1.0×10^{2}
ρ_2	h	15.9	10.5	22.8
γ	h	69.0	19.0	1.5×10^{2}
δ_1	h	38.8	25.4	54.0
δ_2	h	NA	1.0	2.0×10^{2}
ω_1	$cp \cdot h^{-1}$	1.2×10^{7}	1.0×10^{6}	3.0×10^{8}
ω_2	$cp \cdot h^{-1}$	7.9×10^{7}	7.9×10^{6}	6.8×10^{8}
ω_3	$cp \cdot h^{-1}$	1.1×10^{6}	1.6×10^{5}	1.0×10^{7}
ε	$\% \cdot h^{-1}$	5.8	4.0	7.7

The Morris method was first applied to the number of infectious individuals at the theoretical epidemic peak to identify the parameters exerting the strongest influence on the model's outputs. These key parameters were then selected for a second, time-resolved sensitivity analysis designed to assess how their influence evolved throughout the course of the epidemic. The number of infectious individuals at every two-hour time point was used as the model output, with 20 random trajectories and 100 simulations performed for each parameter set. The resulting data were visualized using the "geom_smooth" function from the *ggplot2* package (Wickham, Chang, et al., 2025), applying the LOESS method (Cleveland, 1979) to highlight general temporal trends.

All R scripts (R Core Team, 2023) -including models, ABC approach and sensivity analyses- developed and used in this study are available at: https://gitlab.ifremer.fr/asim/ideal_oshv-1_sweird_model.

RESULTS

Estimation of infection-to-infectiousness time, infectious periods, and shedding rates

The experimental approaches revealed differences between oysters that survived infection and those that succumbed to it **(Supplementary Fig. 2)**. Although the latent period followed a log-normal distribution in both groups, it was longer in surviving oysters (mean ρ_1 = 34.9 hours), than in oysters that died from infection (mean ρ_2 = 14 hours) **(Supplementary Fig. 2A)**. In addition, the log-transformed number of viral particles released per hour followed a normal distribution for non-surviving oysters (ω_2), with a mean corresponding to 6.91×10^7 DNA copies per hour ($cp.h^{-1}$), more than 30 times higher than that of surviving oysters (ω_1), whose log-transformed shedding rate followed a log-normal distribution with a mean value corresponding to 1.89×10^6 $cp.h^{-1}$ **(Supplementary Fig. 2B)**.

Moreover, beyond comparative analyses, these experimental approaches allowed estimating the distribution of other key parameters. The infectious period of oyster that survive infection followed a gamma distribution with a mean of 66.5 hours (γ), the infectious period of alive oyster that succumb to infection followed a log-normal distribution with a mean of 96.7 hours (δ_1), and the log-transformed viral shedding rate of infectious dead oysters was also log-normally distributed, with a mean corresponding to 9.97×10^5 $cp.h^{-1}$ (ω_3).

Estimation of the 50% infectious concentration and virus inactivation rate in seawater

The resulting infection rates as a function of the log-transformed injected viral dose from the third experimental approach **(Supplementary Fig. 1C)** was used to estimate the 50% infectious concentration (*K*) and its 95% confidence interval **(Supplementary Fig. 3A)**. By identifying the x-coordinate on the linear regression corresponding to a 50% infection rate, the 50% infectious dose was estimated to be 2.01×10^3 cp, equivalent to 20.1 $cp.\mu L^{-1}$ given that 100 µL were injected per oyster. The 95% confidence interval was estimated to be $[6.16 \times 10^{-1} : 6.56 \times 10^2]$ $cp.\mu L^{-1}$.

Additionally, the experimental setup implemented to assess the inactivation rate of viral particles in seawater **(Supplementary Fig. 1D)** revealed that oyster mortality (*M*) decreased as the resting time of the contaminated seawater increased **(Supplementary Fig. 3B).** Direct exposure to freshly contaminated seawater results in a 50% mortality rate, whereas a resting period of 2 to 4 hours reduced it to 40%. Moreover, when the contaminated seawater rested for 8 to 16 hours, mortality dropped to around 10%, and no mortality was observed after 20 hours. Then, using the previously estimated *K* value and the observed mortality rates (*M*), the Hill equation was used to infer the concentration of infectious viral particles remaining at each time point (0, 2, 4, 8, 12, 16, and 20 h) **(Supplementary Fig. 3C)**. Linear regression of these estimates against time yielded the slope coefficient **(Supplementary Fig. 3D)** used to estimate the viral particle inactivation rate in seawater under constant and controlled conditions (ε) **(Supplementrary** Fig. 3E**)**. This was estimated to be $5.87\%{\cdot}h^{-1}$ with a 95% interval confidence of $[5.05 : 8.92]$ $\%{\cdot}h^{-1}$.

Optimization of model simulations using ABC-calibration

Parameters estimated from experimental data were used to perform initial model simulations. However these simulations exhibited a temporal delay and underestimated mortality relative to observed data (Fig. 2A). To reduce these discrepancies, an ABC-based approach was therefore used to refine parameters estimates.

A total of more than 9.8×10^4 simulations, distributed over five ABC iterations, were required for the algorithm to converge from the prior distributions to the posterior distributions of all the model parameters **(Supplementary Fig. 4)**. Substantial differences between prior and posterior distributions were observed for several key parameters, based on comparisons of their median values. The most marked difference concerns the viral shedding rate of surviving oysters (ω_1), which increased by 13.7% on the log-transformed scale. Notable decreases are also observed for the concentration inducing 50% infection (K), the infectious period δ_1 and the latent period ρ_2 with median reductions of 65.4%, 57.0%, and 19.7%, respectively. In contrast, other parameters showed limited posterior updating, with median shifts remaining below 15%.

Additionnally, simulations relying on ABC-calibrated parameters showed mortality dynamics that were markedly closer to the observed data than those obtained using experimentally derived parameters (Fig. 2B). These results indicate that the model calibrated using the ABC approach reproduces the observed patterns more accurately than the model using experimentally derived parameters, thereby supporting its validity.

Sensitivity model analysis

The Morris sensitivity analysis performed on the number of infectious individuals at the theoretical peak of the epidemic (t = 19), using ABC-calibrated values (Table 2), revealed clear differences in parameter influence on the model dynamics (Fig. 3A). The shedding rate ω_1 exhibited the largest mean absolute effect (μ_k^*) and was associated with a high standard deviation ($\sigma_k > \sigma$), indicating a strong overall and variable influence of this parameter on the number of infectious individuals at the peak. Other parameters, such as γ, K, Φ, ρ_1, ρ_2 and ω_2 also exhibited substantial mean absolute effects, and were associated with lower standard deviations.

Furthermore, examining how the influence of these parameter variations evolves over time during the simulation revealed distinct trends (Fig. 3B). The early stages of the simulation were primarily driven by parameters ω_1, ω_2 and K. However, after 50 hours of simulation, the influence of these parameters had markedly decreased and had been surpassed by parameters such as Φ, γ and ρ_1 which exhibited a significantly stronger impact at this stage than at the beginning of the simulation. In contrast, the influence of ρ_2 appeared relatively constant throughout the simulation.

DISCUSSION

The experimental approaches developed in this study enabled the estimation of parameters of the proposed model, allowing simulations specifically tailored to the epidemiological dynamics of the OsHV-

1 µVar originating from Marennes-Oléron Bay in small *M. gigas* populations. In addition, combining ABC-based calibration with sensitivity analysis helped to identify the key drivers of epidemic dynamics, while also highlighting parameters that were likely misestimated and reducing discrepancies between observed and simulated data.

Comparison of parameter estimates across OsHV-1 microvariants

The experimental approaches enabled parameter estimations consistent with the literature. For example, considering the case of viral particle inactivation in seawater (ε), precise estimates of this parameter remained until now scarce due to its strong dependence on multiple environmental factors (Vigneron et al., 2004). However, it as been shown on an OsHV-1 microvariant originated from Australia that, starting from viral loads exceeding 10^6 cp.µL^{-1}, a drastic reduction in detectable viral DNA can occur within the first 24 hours, dropping to below 10 cp.µL^{-1} (P. Hick et al., 2016). Although this variant might be genetically and phenotypically different from the OsHV-1 µVar isolated in 2014 in Marennes-Oléron Bay, this observation is consistent with our findings. Indeed, our results show that virus-contaminated seawater no longer causes mortality after 20 hours of resting time, which supports the estimated degradation rate of 5.87% and corresponds to an average viral infectivity period in seawater of approximately 17 hours. Similarly, the estimated concentration required to infect 50% of individuals in the present study ($K \approx 20$ cp.µL^{-1}) is consistent with the literature, as it falls within the same order of magnitude as the value previously estimated for the same variant and used in another model (≈ 80 cp.µL^{-1}) (Ferreira et al., 2021). Additionnaly, our results on the infectious period prior to death (96.7 hours, approximately 4 days), are also consistent with values used for the same parameter in previous modelling studies based on OsHV-1 µVar from other origins (5.8 and 5 days) (Adekunle et al., 2025; Ferreira et al., 2021).

However, certain parameter estimates susbtantially differ from other values reported in the literature. For instance, the shedding rate of oysters that succumb to the infection was estimated at 6.9×10^7 cp.h^{-1} in our study, whereas previous estimates based on an American microvariant reported a value of $\approx 3 \times 10^6$ cp.h^{-1} (Ferreira et al., 2021). Although these differences may be explained by several factors, including environmental conditions and the oyster stocks used in the experiments, they may also reflect genetic and phenotypic variations among viruses from distinct origins, known to induce distinct host responses and, consequently, distinct shedding rates (Agnew-Camiener et al., 2026). This example support the development of a model framework that can be calibrated to the specific viral variant under study, thereby improving predictive performance for viral dynamics.

Discrepencies due to model assumptions addressed using ABC approach

Although the experimental approaches implemented provided parameter estimates that were mostly consistent with the existing literature, the simulations outputs nevertheless differed from the observed

mortality kinetics data. The simulations using parameters calibrated using experimental data resulted in a mortality curve characterized by slower kinetics than those observed in validation data. Indeed, simulated mortality stabilizing only after approximately 500 hours, whereas the observed mortality plateaued around 100 hours, which is in line with previous experimental infections on microvariant form the same origin (Schikorski, Renault, et al., 2011b). This mismatch may, in part, be attributed to the simplifying assumptions made during model implementation. In particular, the assumption that viral DNA quantified by qPCR reflects the number of infectious viral particles may bias parameter estimation, potentially leading to an overestimation of key parameters such as shedding rates. This may artificially accelerate the simulated epidemiological dynamics, even though these ultimately appear slower than those observed in the empirical data. Moreover, since the estimated 50% infectious concentration (K) was derived from PMA-qPCR data and is therefore not as affected by this overestimation (Renault et al., 2024), it may introduce a shift that could explain the differences observed in the infection kinetics. Additionally, this parameter, like several others, was estimated from experimental infections performed by injection and therefore does not account for the natural route of viral entry, which may have led to a misestimation of the number of viral particles required to initiate infection.

Indeed, results of the ABC approach indicate that several adjustments were needed for a majority of the estimated parameter values, and most importantly for the key drivers of the transmission dynamics highlighted by the sensitivity analysis. This is, for example, the case for parameter K, which was identified as an important parameter of the model and as potentially overestimated, with a posterior median adjusted to a value approximately 3 times lower than the prior median. This is also the case for the viral shedding rate of oysters that survive infection (ω_1), whose posterior median was more than 7 times higher than the prior median. Then, by refining posterior distributions using validation data, the ABC approach therefore helps adjust parameter values and produce simulations that more closely match the observed data, thereby improving predictions of OsHV-1 µVar infection dynamics in a local *M. gigas* population at an hourly time scale.

Key drivers of OsHV-1 uVar dynamics

The sensitivity analysis, conducted using parameters ranges resulting from the ABC approach, revealed that all model parameters influence the transmission dynamics, with their relative impact varying throughout the course of the epidemic. However, some parameters stand out because of their particularly strong influence. This is the case for the viral shedding rate of recovering oysters (ω_1), which emerged as the main driver of the epidemiological dynamics. This is consistent with previous studies showing the central role of shedding in infection spread and epidemic progression (Faisal et al., 2019; Hershberger et al., 2010). Sensitivity analyses also highlighted the strong influence of the concentration causing 50% infection (K) in viral dynamics during the early stages of the simulation. This finding supports the high transmissibility of OsHV-1 consistent with an estimated 50% infection dose of 2×10^3 cp, which appears lower than that reported for other herpesviruses, such as HSV-2, for which transmission is considered unlikely below 10^4 cp (Schiffer et al., 2014).

Additionally, experimental approaches revealed distinct parameters values between oysters that survived infection and oysters that succumbed to it. These results emphasize the crucial importance of integrating both phenotypes, and thus both epidemiological pathways, into the modeling approach to accurately capture the viral transmission dynamics (Segarra, Mauduit, et al., 2014). Moreover, these observations, together with the sensitivity analysis, also underscore the crucial role of oyster survival probability associated with potential genetic resistance (Dégremont, Garcia, et al., 2015) and highlight the need to explore how its variation influence viral dynamics and the potential outcomes of selective breeding programs.

Further developments towards spatial and biologically realistic modeling

The dynamics of OsHV-1 µVar transmission within a *M. gigas* population constitute a multifactorial biological process, requiring simplifying approximations to enable effective modelling. However, incorporating key biological, environmental and anthropogenic factors is essential to enhance the predictive accuracy of such a model and to extend its relevance beyond controlled experimental settings, allowing for its application under natural conditions.

Developing a realistic model requires accounting for variations in oyster farming density, a major driver of viral replication and epidemic spread. Oyster densities fluctuate seasonally in relation to production cycles and are influenced by natural recruitment and the introduction of hatchery-produced spats or juveniles from other regions **(**Fig. 4A**)** (Lupo et al., 2016), as well as natural mortality **(**Fig. 4B**)**. Additionnaly, as studies have reported OsHV-1 DNA and protein in asymptomatic oyster (Arzul et al., 2002; Segarra et al., 2016) together with viral particle shedded from previously recovered oysters (Degremont & Benabdelmouna, 2014), it is therefore strongly suspected that OsHV-1 may exhibit a persistance phase **(**Fig. 4C**)**. Then, under favorable environmental conditions, recovered oysters may become infectious again, impacting the number of infectious individuals and therefore the dynamics of the virus. Including such a multi-annual dimension would allow recovered oysters to transition either to a persistence compartment, representing individuals that still carry the virus, or to the susceptible state **(**Fig. 4D**)**, representing young oysters that remain vulnerable to infection, with newly settled or hatchery-produced spat.

Incorporating environmental factors is also a key step in developing a realistic model, as they influence both the virus and its host **(**Fig. 4E**)**. Temperature for example is a critical driver of infection dynamics, with a specific range facilitating viral infection and spread (Delisle et al., 2018; Renault et al., 2014). It's also the case for salinity, pH, and turbidity, which are known to influence the stability of herpesviruses in aquatic environments (Dayaram et al., 2017) and have been shown to affect OsHV-1 infection dynamics (Fuhrmann et al., 2019; Renault et al., 2014; Soletchnik et al., 2007). In addition, environmental conditions can affect filtration activity of oysters, thereby increasing the infection risk (Pousse et al., 2018), but also impact the oyster microbiome, a key determinant of sensitivity to OsHV-1 µVar infection (Pathirana et al., 2017). Moreover, phenotypic differences in infection outcome varies also with developmental stage and

individual size (P. M. Hick et al., 2018), which represent key epidemiological parameters that should be also explicitly considered in future developments of a climate-sensitive model (Fig. 4F).

Other factors also play a key role in the epidemiological dynamics of OsHV-1 by exerting a direct influence on the virus itself. By affecting viral spread and transmission, hydrodynamics should be carefully considered especially in the context spatial modelling (Fig. 4G) (Lupo et al., 2019; Murray, 2013). Additionally, alternative transmission pathways, such as other host species, could be considered as different virus OsHV-1 genotypes are reported in other bivalve species worldwide and the virus appears as evolving quite rapidly for a herpesvirus (Delmotte et al., 2022; Morga et al., 2021). Nevertheless, existing evidence suggests that potential alternative hosts are limited (Camille Pelletier, 2024), and other filter-feeders appear to have no significant impact on viral concentrations (Pernet et al., 2021).

CONCLUSION

By combining experimental data, ABC-based approach, and sensitivity analysis, we provide an calibrated framework for investigating the epidemiological dynamics of OsHV-1 µVar within a local *M. gigas* population. Beyond reproducing observed infection dynamics, this modeling framework serves as a powerful tool to identify the key drivers shaping epidemic trajectories, notably highlighting the critical role of inter-individual variability in host ability to survive infection and viral shedding rates, particularly during the early stages of the epidemic. Building on this foundation, extending the model toward a spatially explicit framework represents a key next step. Incorporating hydrodynamics, farming practices, and environmentally driven variability in the virus-host relationship would enable a more realistic representation of OsHV-1 transmission, providing a valuable tool to support decision-making and mitigate the impact of the virus.

Declarations

Author Contribution

BM, NF, BP, TR and MJ designed and carried out the experimental approaches described in this study. JT analysed the data and integrated them into a modelling approach developed by JT, CL and MJ. JT and MJ drafted the manuscript, figures and tables, with substantial contributions from IA. All authors reviewed the manuscript.

Acknowledgement

The authors acknowledge the French National Research Agency (ANR) for funding Jules Trillaud's PhD. We also thank Mickael Mege, Fabrice Pernet and Jacqueline Le Grand for their contribution to the experimental work used for model parameter estimation.

Data Availability

The dataset and codes supporting the conclusions of this article are available at: https://gitlab.ifremer.fr/asim/ideal_oshv-1_sweird_model

References

1. Adekunle FO, Bidegain G, Ben-Horin T (2025) Coculture with Eastern oysters is unlikely to reduce OsHV-1 impacts to farmed Pacific oysters: A modelling approach. Aquaculture Rep 40:102567. https://doi.org/10.1016/J.AQREP.2024.102567
2. Agnew-Camiener MV, Burge CA, Schreier HJ, Parikh MP (2026) Shedding of OsHV-1 from infected Pacific oysters depends on viral variant. *Philosophical Transactions of the Royal Society B: Biological Sciences*, *381*(1945). https://doi.org/10.1098/RSTB.2025.0047
3. Akaike H (1974) A New Look at the Statistical Model Identification. IEEE Trans Autom Control 19(6):716–723. https://doi.org/10.1109/TAC.1974.1100705
4. Alfaro AC, Nguyen TV, Merien F (2019) The complex interactions of Ostreid herpesvirus 1, Vibrio bacteria, environment and host factors in mass mortality outbreaks of Crassostrea gigas. Reviews Aquaculture 11(4):1148–1168. https://doi.org/10.1111/RAQ.12284
5. Arzul I, Renault T, Thébault A, Gérard A (2002) Detection of oyster herpesvirus DNA and proteins in asymptomatic Crassostrea gigas adults. Virus Res 84(1–2):151–160. https://doi.org/10.1016/S0168-1702(02)00007-2
6. Azéma P, Lamy JB, Boudry P, Renault T, Travers MA, Dégremont L (2017) Genetic parameters of resistance to Vibrio aestuarianus, and OsHV-1 infections in the Pacific oyster, Crassostrea gigas, at three different life stages. Genet Selection Evol 49(1):1–16. https://doi.org/10.1186/S12711-017-0297-2/FIGURES/4
7. Beaumont MA, Zhang W, Balding DJ (2002) Approximate Bayesian Computation in Population Genetics. Genetics 162(4):2025–2035. https://doi.org/10.1093/GENETICS/162.4.2025
8. Bidegain G, Powell EN, Klinck JM, Hofmann EE, Ben-Horin T, Bushek D, Ford SE, Munroe DM, Guo X (2017) Modeling the transmission of Perkinsus marinus in the Eastern oyster Crassostrea virginica. Fish Res 186:82–93. https://doi.org/10.1016/J.FISHRES.2016.08.006
9. Botta R, Asche F, Borsum JS, Camp EV (2020) A review of global oyster aquaculture production and consumption. Mar Policy 117:103952. https://doi.org/10.1016/J.MARPOL.2020.103952
10. Camille Pelletier (2024) *Diversité et évolution de l'Ostreid Herpesvirus type 1* [Université de La Rochelle]. https://doi.org/10.34894/VQ1DJA
11. Cleveland WS (1979) Robust locally weighted regression and smoothing scatterplots. J Am Stat Assoc 74(368):829–836. https://doi.org/10.1080/01621459.1979.10481038
12. Csilléry K, Blum MGB, Gaggiotti OE, François O (2010) Approximate Bayesian Computation (ABC) in practice. Trends Ecol Evol 25(7):410–418.

https://doi.org/10.1016/J.TREE.2010.04.001/ASSET/0F6DB589-C368-4A08-B491-70C158136012/MAIN.ASSETS/GR1.JPG

13. Davison AJ, Trus BL, Cheng N, Steven A, Watson MS, Cunningham C, Le Deuff RM, Renault T (2005) A novel class of herpesvirus with bivalve hosts. J Gen Virol 86(1):41–53. https://doi.org/10.1099/VIR.0.80382-0/CITE/REFWORKS
14. Dayaram A, Franz M, Schattschneider A, Damiani AM, Bischofberger S, Osterrieder N, Greenwood AD (2017) Long term stability and infectivity of herpesviruses in water. *Scientific Reports 2017 7:1*, *7*(1), 1–10. https://doi.org/10.1038/srep46559
15. Dégremont L (2011) Evidence of herpesvirus (OsHV-1) resistance in juvenile Crassostrea gigas selected for high resistance to the summer mortality phenomenon. Aquaculture 317(1–4):94–98. https://doi.org/10.1016/J.AQUACULTURE.2011.04.029
16. Dégremont L, Bédier E, Boudry P (2010) Summer mortality of hatchery-produced Pacific oyster spat (Crassostrea gigas). II. Response to selection for survival and its influence on growth and yield. Aquaculture 299(4):21–29. https://doi.org/10.1016/j.aquaculture.2009.11.017
17. Degremont L, Benabdelmouna A (2014) Mortality associated with OsHV-1 in spat Crassostrea gigas: role of wild-caught spat in the horizontal transmission of the disease. Aquacult Int 22(6):1767–1781. https://doi.org/10.1007/S10499-014-9781-7/TABLES/3
18. Dégremont L, Garcia C, Allen SK (2015) Genetic improvement for disease resistance in oysters: A review. J Invertebr Pathol 131:226–241. https://doi.org/10.1016/J.JIP.2015.05.010
19. Dégremont L, Lamy JB, Pépin JF, Travers MA, Renault T (2015) New Insight for the Genetic Evaluation of Resistance to Ostreid Herpesvirus Infection, a Worldwide Disease, in Crassostrea gigas. PLoS ONE 10(6). https://doi.org/10.1371/JOURNAL.PONE.0127917
20. Dégremont L, Morga B, Trancart S, Pépin JF (2016) Resistance to OsHV-1 infection in crassostrea gigas larvae. Front Mar Sci 3(FEB):178314. https://doi.org/10.3389/FMARS.2016.00015/BIBTEX
21. Dégremont L, Nourry M, Maurouard E (2015) Mass selection for survival and resistance to OsHV-1 infection in Crassostrea gigas spat in field conditions: response to selection after four generations. Aquaculture 446:111–121. https://doi.org/10.1016/J.AQUACULTURE.2015.04.029
22. Delisle L, Petton B, Burguin JF, Morga B, Corporeau C, Pernet F (2018) Temperature modulate disease susceptibility of the Pacific oyster Crassostrea gigas and virulence of the Ostreid herpesvirus type 1. Fish Shellfish Immunol 80:71–79. https://doi.org/10.1016/J.FSI.2018.05.056
23. Delmotte J, Pelletier C, Morga B, Galinier R, Petton B, Lamy JB, Kaltz O, Avarre JC, Jacquot M, Montagnani C, Escoubas JM (2022) Genetic diversity and connectivity of the Ostreid herpesvirus 1 populations in France: A first attempt to phylogeographic inference for a marine mollusc disease. Virus Evol 8(1):veac039. https://doi.org/10.1093/VE/VEAC039
24. Delomas TA, Hollenbeck CM, Matt JL, Thompson NF (2023) Evaluating cost-effective genotyping strategies for genomic selection in oysters. Aquaculture 562:738844. https://doi.org/10.1016/J.AQUACULTURE.2022.738844

25. Doeschl-Wilson AB (2011) The role of mathematical models of host–pathogen interactions for livestock health and production – a review*. Animal 5(6):895–910. https://doi.org/10.1017/S1751731110002557
26. Efron B, Tibshirani RJ (1994) An Introduction to the Bootstrap. In *An Introduction to the Bootstrap*. Chapman and Hall/CRC. https://doi.org/10.1201/9780429246593/INTRODUCTION-BOOTSTRAP-BRADLEY-EFRON-TIBSHIRANI
27. EFSA (2010) Scientific Opinion on the increased mortality events in Pacific oysters, Crassostrea gigas. EFSA J 8(11):1894. https://doi.org/10.2903/J.EFSA.2010.1894
28. Faisal M, Purbayu M, Shavalier MA, Marsh TL, Loch TP (2019) Shedding of the Salmonid Herpesvirus-3 by Infected Lake Trout (Salvelinus namaycush). Viruses 2019 11(7):580. https://doi.org/10.3390/V11070580. *11*
29. FAO (2024) The State of World Fisheries and Aquaculture 2024. In *The State of World Fisheries and Aquaculture 2024*. FAO. https://doi.org/10.4060/CD0683EN
30. Ferreira JG, Taylor NGH, Cubillo A, Lencart-Silva J, Pastres R, Bergh Ø, Guilder J (2021) An integrated model for aquaculture production, pathogen interaction, and environmental effects. Aquaculture 536:736438. https://doi.org/10.1016/J.AQUACULTURE.2021.736438
31. Fox J, Weisberg S, Price B (2024) Companion to Applied Regression [R package car version 3.1-3]. CRAN: Contributed Packages. https://doi.org/10.32614/CRAN.PACKAGE.CAR
32. Friedman CS, Reece KS, Wippel BJT, Agnew MV, Dégremont L, Dhar AK, Kirkland P, MacIntyre A, Morga B, Robison C, Burge CA (2020) Unraveling concordant and varying responses of oyster species to Ostreid Herpesvirus 1 variants. Sci Total Environ 739:139752. https://doi.org/10.1016/J.SCITOTENV.2020.139752
33. Fuhrmann M, Richard G, Quéré C, Petton B, Pernet F (2019) Low pH reduced survival of the oyster Crassostrea gigas exposed to the Ostreid herpesvirus 1 by altering the metabolic response of the host. Aquaculture 503:167–174. https://doi.org/10.1016/J.AQUACULTURE.2018.12.052
34. Garcia C, Thébault A, Dégremont L, Arzul I, Miossec L, Robert M, Chollet B, François C, Joly JP, Ferrand S, Kerdudou N, Renault T (2011) Ostreid herpesvirus 1 detection and relationship with Crassostrea gigas spat mortality in France between 1998 and 2006. Vet Res 42(1). https://doi.org/10.1186/1297-9716-42-73
35. Giménez-Romero À, Grau A, Hendriks IE, Matias MA (2021) Modelling parasite-produced marine diseases: The case of the mass mortality event of Pinna nobilis. Ecol Model 459:109705. https://doi.org/10.1016/J.ECOLMODEL.2021.109705
36. Girard S, Pérez Agúndez JA (2014) The effects of the oyster mortality crisis on the economics of the shellfish farming sector: Preliminary review and prospects from a case study in Marennes-Oleron Bay (France). Mar Policy 48:142–151. https://doi.org/10.1016/J.MARPOL.2014.03.024
37. Green TJ, Vergnes A, Montagnani C, De Lorgeril J (2016) Distinct immune responses of juvenile and adult oysters (Crassostrea gigas) to viral and bacterial infections. Vet Res 47(1):72. https://doi.org/10.1186/S13567-016-0356-7/FIGURES/5

38. Hershberger P, Gregg J, Grady C, Collins R, Winton J (2010) Kinetics of viral shedding provide insights into the epidemiology of viral hemorrhagic septicemia in Pacific herring. Mar Ecol Prog Ser 400:187–193. https://doi.org/10.3354/MEPS08420
39. Hick P, Evans O, Looi R, English C, Whittington RJ (2016) Stability of Ostreid herpesvirus-1 (OsHV-1) and assessment of disinfection of seawater and oyster tissues using a bioassay. Aquaculture 450:412–421. https://doi.org/10.1016/J.AQUACULTURE.2015.08.025
40. Hick PM, Evans O, Rubio A, Dhand NK, Whittington RJ (2018) Both age and size influence susceptibility of Pacific oysters (Crassostrea gigas) to disease caused by Ostreid herpesvirus-1 (OsHV-1) in replicated field and laboratory experiments. Aquaculture 489:110–120. https://doi.org/10.1016/J.AQUACULTURE.2018.02.013
41. Hill A, Hill A, Paganini-Hill A (1910) The possible effects of the aggregation of the molecules of haemoglobin on its dissociation curves. J Physiol
42. Hwang JY, Park JJ, Yu HJ, Hur YB, Arzul I, Couraleau Y, Park MA (2013) Ostreid herpesvirus 1 infection in farmed Pacific oyster larvae Crassostrea gigas (Thunberg) in Korea. J Fish Dis 36(11):969–972. https://doi.org/10.1111/JFD.12093
43. Iooss B, Da Veiga S, Janon A, Pujol G (2025) Global Sensitivity Analysis of Model Outputs and Importance Measures [R package sensitivity version 1.30.2]. CRAN: Contributed Packages. https://doi.org/10.32614/CRAN.PACKAGE.SENSITIVITY
44. Jenkins C, Hick P, Gabor M, Spiers Z, Fell SA, Gu X, Read A, Go J, Dove M, O'Connor W, Kirkland PD, Frances J (2013) Identification and characterisation of an ostreid herpesvirus-1 microvariant (OsHV-1 µ-var) in Crassostrea gigas (Pacific oysters) in Australia. Dis Aquat Organ 105(2):109–126. https://doi.org/10.3354/DAO02623
45. Keeling MJ, Rohani P (2008) Modeling Infectious Diseases in Humans and Animals. Princeton University Press. https://doi.org/10.2307/J.CTVCM4GK0
46. Keeling SE, Brosnahan CL, Williams R, Gias E, Hannah M, Bueno R, McDonald WL, Johnston C (2014) New Zealand juvenile oyster mortality associated with ostreid herpesvirus 1-an opportunistic longitudinal study. Dis Aquat Organ 109(3):231–239. https://doi.org/10.3354/DAO02735
47. Kermack W 0, Mckendrick AG (1927) A contribution to the mathematical theory of epidemics. *Proceedings of the Royal Society of London. Series A, Containing Papers of a Mathematical and Physical Character*, *115*(772), 700–721. https://doi.org/10.1098/RSPA.1927.0118
48. Lenormand M, Jabot F, Deffuant G (2013) Adaptive approximate Bayesian computation for complex models. Comput Stat 28(6):2777–2796. https://doi.org/10.1007/S00180-013-0428-3/FIGURES/5
49. Lupo C, Ezanno P, Arzul I, Garcia C, Jadot C, Joly J-P, Renault T, Bareille N (2016) How network analysis of oyster movements can improve surveillance and control programs of infectious diseases? Front Veterinary Sci 3:np. https://doi.org/10.3389/CONF.FVETS.2016.02.00044
50. Lupo C, Travers MA, Tourbiez D, Barthélémy CF, Beaunée G, Ezanno P (2019) Modeling the transmission of vibrio aestuarianus in pacific oysters using experimental infection data. Front Veterinary Sci 6(MAY):427547. https://doi.org/10.3389/FVETS.2019.00142/BIBTEX

51. Marques JAL, Gois FNB, Xavier-Neto J, Fong SJ (2021) Epidemiology Compartmental Models—SIR, SEIR, and SEIR with Intervention. SpringerBriefs Appl Sci Technol 15–39. https://doi.org/10.1007/978-3-030-61913-8_2
52. Morga B, Jacquot M, Pelletier C, Chevignon G, Dégremont L, Biétry A, Pepin JF, Heurtebise S, Escoubas JM, Bean TP, Rosani U, Bai CM, Renault T, Lamy JB (2021) Genomic Diversity of the Ostreid Herpesvirus Type 1 Across Time and Location and Among Host Species. Front Microbiol 12:711377. https://doi.org/10.3389/FMICB.2021.711377/TEXT
53. Morris MD (1991) Factorial Sampling Plans for Preliminary Computational Experiments. Technometrics, *33*(2)
54. Murray AG (2013) Epidemiology of the spread of viral diseases under aquaculture. Curr Opin Virol 3(1):74–78. https://doi.org/10.1016/J.COVIRO.2012.11.002
55. Murray AG, O'Callaghan M, Jones B (2001) A model of transmission of a viral epidemic among schools within a shoal of pilchards. Ecol Model 144(2–3):245–259. https://doi.org/10.1016/S0304-3800(01)00375-1
56. Oehlert GW (1992) A Note on the Delta Method. Am Stat 46(1):27. https://doi.org/10.2307/2684406
57. Pathirana E, Fuhrmann M, Whittington R, Hick P (2017) Influence of environment on the pathogenesis of Ostreid herpesvirus-1 (OsHV-1) infections in Pacific oysters (Crassostrea gigas) through differential microbiome responses. Heliyon e02101. https://doi.org/10.1016/j.heliyon.2019.e02101
58. Pepin JF, Riou A, Renault T (2008) Rapid and sensitive detection of ostreid herpesvirus 1 in oyster samples by real-time PCR. J Virol Methods 149(2):269–276. https://doi.org/10.1016/J.JVIROMET.2008.01.022
59. Pernet F, Lugue K, Petton B (2021) *Competition for food reduces disease susceptibility in a marine invertebrate*. https://doi.org/10.1002/ecs2.3435ï
60. Pernet F, Lupo C, Bacher C, Whittington RJ (2016) Infectious diseases in oyster aquaculture require a new integrated approach. Philosophical Trans Royal Soc B: Biol Sci 371(1689). https://doi.org/10.1098/RSTB.2015.0213
61. Pousse É, Flye-Sainte-Marie J, Alunno-Bruscia M, Hégaret H, Jean F (2018) Sources of paralytic shellfish toxin accumulation variability in the Pacific oyster Crassostrea gigas. Toxicon 144:14–22. https://doi.org/10.1016/J.TOXICON.2017.12.050
62. R Core Team (2023) *R: The R Project for Statistical Computing*. https://www.r-project.org/
63. Renault T (2024) Malacoherpesviruses of mollusks. Aquaculture Virol 655–670. https://doi.org/10.1016/B978-0-323-91169-6.00003-0
64. Renault T, Bouquet AL, Maurice JT, Lupo C, Blachier P (2014) Ostreid herpesvirus 1 infection among Pacific oyster (Crassostrea gigas) Spat: relevance of water temperature to virus replication and circulation prior to the onset of mortality. Appl Environ Microbiol 80(17):5419–5426. https://doi.org/10.1128/AEM.00484-14

65. Renault T, Cochennec N, Le Deuff RM, Chollet B (1994) HERPES-LIKE VIRUS INFECTING JAPANESE OYSTER (CRASSOSTREA GIGAS) SPAT. Bull Eur Ass Fish Pathol 14(2):64
66. Renault T, Deuff RL, Cochennec N, Chollet B, Maffart P (1995) Herpes-like viruses associated with high mortality levels in larvae and spat of Pacific oysters, Crassostrea gigas: a comparative study, the thermal effects on virus detection in hatchery-reared larvae, reproduction of the disease in axenic larvae. *Veterinary Research*
67. Renault T, Faury N, Morga B (2024) Propidium monoazide PCR, a method to determine OsHV-1 undamaged capsids and to estimate virus Lethal Dose 50. Virus Res 340:199307. https://doi.org/10.1016/J.VIRUSRES.2023.199307
68. Renault T, Le Deuff RM, Cochennec N, Maffart P (1994) *Herpesviruses associated with mortalities among Pacifie oyster, Crassostrea gigas, in France · Comparative study*
69. Renault T, Moreau P, Faury N, Pepin J-F, Segarra A, Webb S (2012) Analysis of clinical ostreid herpesvirus 1 (Malacoherpesviridae) specimens by sequencing amplified fragments from three virus genome areas. J Virol 86(10):5942–5947. https://doi.org/10.1128/JVI.06534-11
70. Salama NKG, Murray AG (2013) A comparison of modelling approaches to assess the transmission of pathogens between Scottish fish farms: The role of hydrodynamics and site biomass. Prev Vet Med 108(4):285–293. https://doi.org/10.1016/J.PREVETMED.2012.11.005
71. Schiffer JT, Mayer BT, Fong Y, Swan DA, Wald A (2014) Herpes simplex virus-2 transmission probability estimates based on quantity of viral shedding. J Royal Soc Interface 11(95). https://doi.org/10.1098/RSIF.2014.0160
72. Schikorski D, Faury N, Pepin J-F, Saulnier D, Tourbiez D, Renault T, Pepin J-F, Saulnier D, Tourbiez D, Renault T (2011) Experimental ostreid herpesvirus 1 infection of the Pacific oyster Crassostrea gigas: Kinetics of virus DNA detection by q-PCR in seawater and in oyster samples. Virus Res 155(1):28–34. https://doi.org/10.1016/J.VIRUSRES.2010.07.031
73. Schikorski D, Renault T, Saulnier D, Faury N, Moreau P, Pépin JF (2011a) Experimental infection of Pacific oyster Crassostrea gigas spat by ostreid herpesvirus 1: demonstration of oyster spat susceptibility. Vet Res 42(1):27. https://doi.org/10.1186/1297-9716-42-27
74. Schikorski D, Renault T, Saulnier D, Faury N, Moreau P, Pépin JF (2011b) Experimental infection of Pacific oyster Crassostrea gigas spat by ostreid herpesvirus 1: demonstration of oyster spat susceptibility. Vet Res 42(1). https://doi.org/10.1186/1297-9716-42-27
75. Segarra A (2014) *Etude des interactions hôte/virus chez l'huître creuse Crassostrea gigas et son virus Ostreid herpesvirus 1*. https://archimer.ifremer.fr/doc/00252/36297/
76. Segarra A, Baillon L, Faury N, Tourbiez D, Renault T (2016) Detection and distribution of ostreid herpesvirus 1 in experimentally infected Pacific oyster spat. J Invertebr Pathol 133:59–65. https://doi.org/10.1016/J.JIP.2015.11.013
77. Segarra A, Baillon L, Tourbiez D, Benabdelmouna A, Faury N, Bourgougnon N, Renault T (2014) Ostreid herpesvirus type 1 replication and host response in adult Pacific oysters, Crassostrea gigas. Vet Res 45(1):103. https://doi.org/10.1186/S13567-014-0103-X/FIGURES/6

78. Segarra A, Mauduit F, Faury N, Trancart S, Dégremont L, Tourbiez D, Haffner P, Barbosa-Solomieu V, Pépin JF, Travers MA, Renault T (2014) Dual transcriptomics of virus-host interactions: comparing two Pacific oyster families presenting contrasted susceptibility to ostreid herpesvirus 1. BMC Genomics 15(1). https://doi.org/10.1186/1471-2164-15-580
79. Segarra A, Pépin JF, Arzul I, Morga B, Faury N, Renault T (2010) Detection and description of a particular Ostreid herpesvirus 1 genotype associated with massive mortality outbreaks of Pacific oysters, Crassostrea gigas, in France in 2008. Virus Res 153(1):92–99. https://doi.org/10.1016/J.VIRUSRES.2010.07.011
80. Siettos CI, Russo L (2013) Mathematical modeling of infectious disease dynamics. Virulence 4(4):295–306. https://doi.org/10.4161/VIRU.24041
81. Soletchnik P, Ropert M, Mazurié J, Fleury G, P., Le Coz F (2007) coasts France Aquaculture 271(1–4):384–400. https://doi.org/10.1016/J.AQUACULTURE.2007.02.049. Relationships between oyster mortality patterns and environmental data from monitoring databases along the
82. Tang L, Zhou Y, Wang L, Purkayastha S, Zhang L, He J, Wang F, Song PXK (2020) A Review of Multi-Compartment Infectious Disease Models. Int Stat Rev 88(2):462–513. https://doi.org/10.1111/INSR.12402
83. Vigneron V, Solliec G, Montanie H, Renault T, Montanie H, Renault T (2004) Detection of ostreid herpesvirus 1 (OsHV-1) DNA in seawater by PCR: influence of water parameters in bioassays. Dis Aquat Organ 62(1–2):35–44. https://archimer.ifremer.fr/doc/00000/2909/
84. Webb SC, Fidler A, Renault T (2007) Primers for PCR-based detection of ostreid herpes virus-1 (OsHV-1): Application in a survey of New Zealand molluscs. Aquaculture 272(1–4):126–139. https://doi.org/10.1016/J.AQUACULTURE.2007.07.224
85. Wickham H (2025) Flexibly Reshape Data: A Reboot of the Reshape Package [R package reshape2 version 1.4.5]. CRAN: Contributed Packages. https://doi.org/10.32614/CRAN.PACKAGE.RESHAPE2
86. Wickham H, Chang W, Henry L, Pedersen TL, Takahashi K, Wilke C, Woo K, Yutani H, Dunnington D, van den Brand T (2025) Create Elegant Data Visualisations Using the Grammar of Graphics [R package ggplot2 version 4.0.0]. CRAN: Contributed Packages. https://doi.org/10.32614/CRAN.PACKAGE.GGPLOT2
87. Wickham H, François R, Henry L, Müller K, Vaughan D (2014) dplyr: A Grammar of Data Manipulation. CRAN: Contributed Packages. https://doi.org/10.32614/CRAN.PACKAGE.DPLYR
88. Wickham H, Vaughan D, Girlich M (2025) Tidy Messy Data [R package tidyr version 1.3.2]. CRAN: Contributed Packages. https://doi.org/10.32614/CRAN.PACKAGE.TIDYR
89. Wu J, Dhingra R, Gambhir M, Remais JV (2013) Sensitivity analysis of infectious disease models: methods, advances and their application. J Royal Soc Interface 10(86). https://doi.org/10.1098/RSIF.2012.1018

Figures

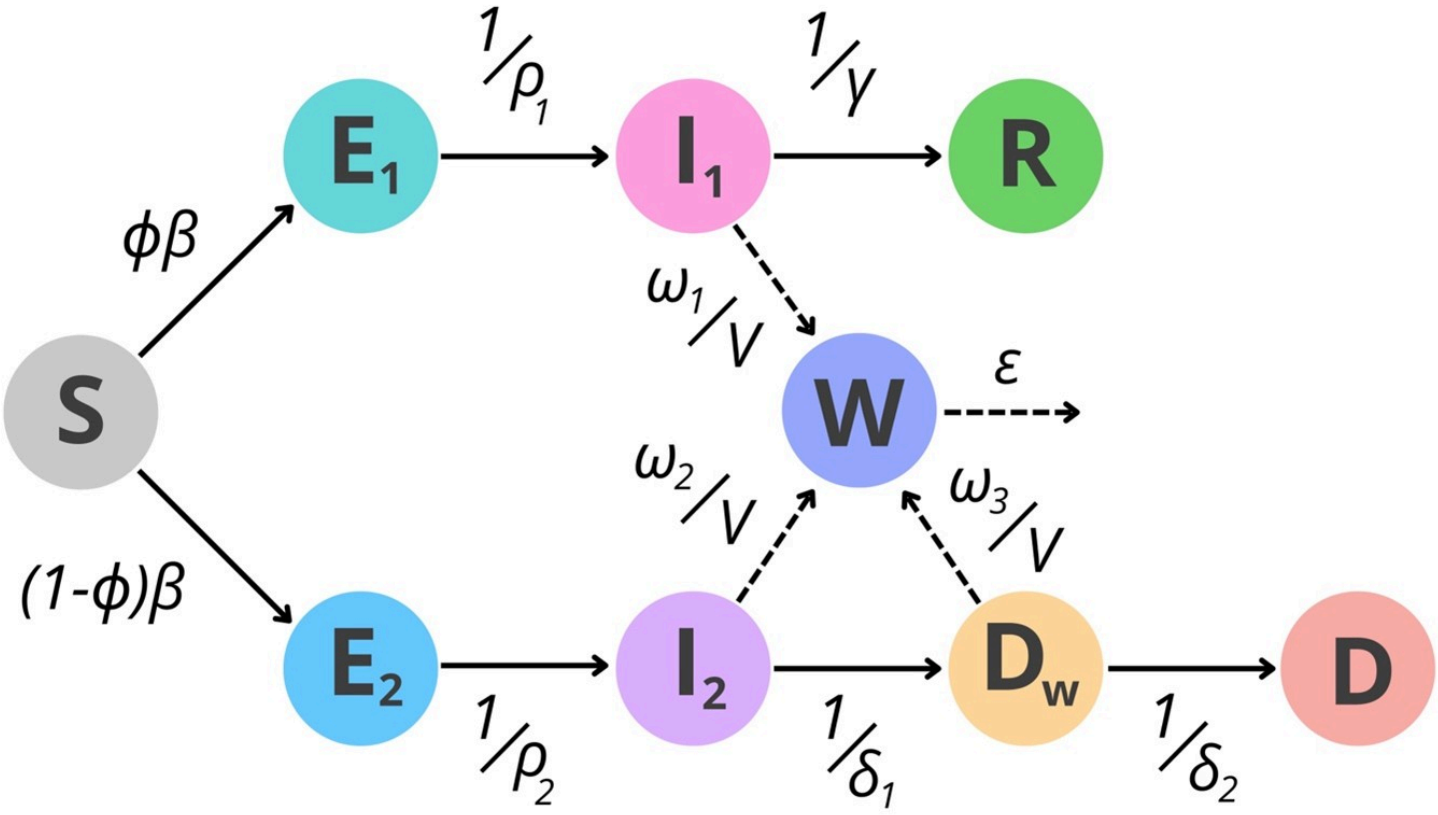

Figure 1

Developed SWEIRD compartmental model.

Possible oyster states include susceptible (S); exposed and infectious oysters that will survive (E_1 and I_1) or succumb to infection (E_2 and I_2); recovered (R); dead shedding (D_w) and dead non-shedding oysters (D). W denotes the viral concentration in seawater. Solid arrows represent oyster transitions, whereas dashed arrows represent virus dynamics. Model parameters are Φ (survival probability); β (probability of infection); ρ_1 and ρ_2 (latent periods); γ, δ_1 and δ_2 (infectious periods); ω_1, ω_2 and ω_3 (shedding rates); ε (viral inactivation rate); and V (seawater volume).

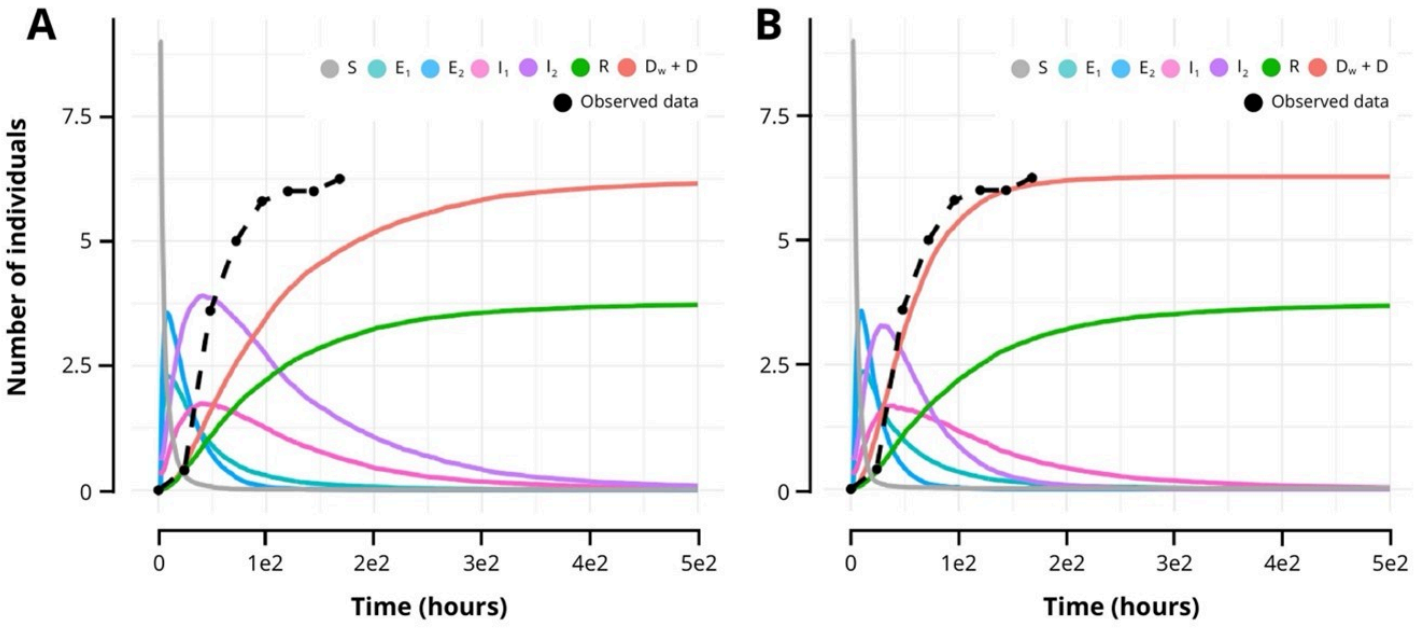

Figure 2

Impact of ABC calibration on model performance.

(A) Mean agregation of 1,000 simulations outputs using estimation of parameters from experimental approaches. (B) Mean agregation of 1,000 simulations outputs using parameters calibrated from the ABC approach.

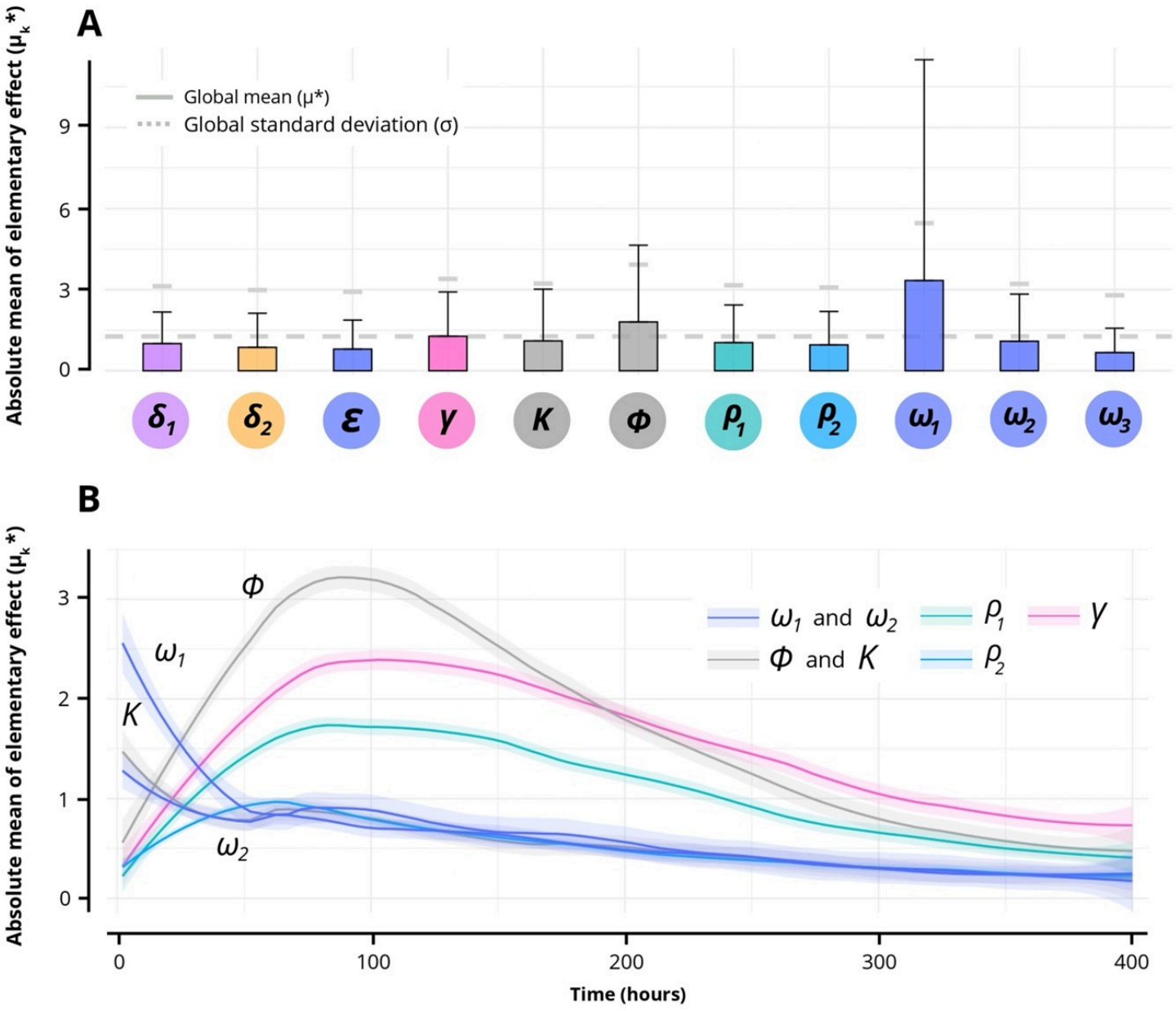

Figure 3

SWEIRD model sensitivity analysis.

(A) Morris sensitivity analysis applied to assess the individual effect of each parameter on the number of infected individuals at t = 19 hours. Elementary effects were combined across the random trajectories using the absolute mean effect on the model output for each parameter (μ_k*). (B) Morris sensitivity analysis was performed at 2-hour intervals throughout the simulation to assess the individual effect of each parameter on the number of infected individuals.

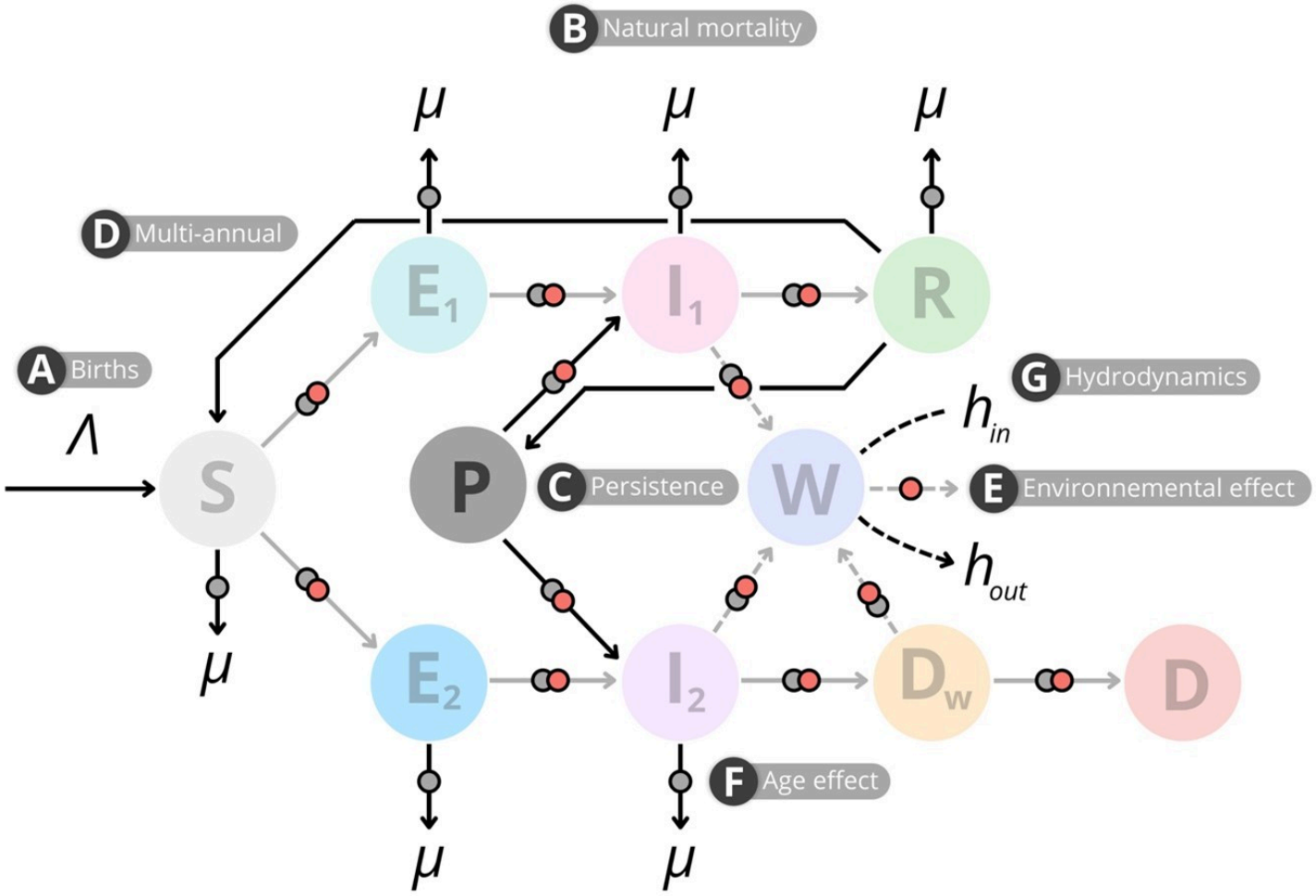

Figure 4

Perspectives for further biologically realistic developments of the SWEIRD model

(A) **Addition of oysters originating from natural settlement or hatchery production**. (B) **Natural mortality.** (C) **Viral persistence in**previously infected and recovered oysters. (D) Multi-year dynamics, allowing recovered oysters to become suceptible again. (E) **Effects of environmental factors**. (F) **Influence of individual development stage**. (G) Hydrodynamic processes influencing local viral concentration.

Supplementary Files

This is a list of supplementary files associated with this preprint. Click to download.

- SUPPLEMENTARYFIGURES.docx